

SIMULATION OF ELECTRON BUNCH SHAPING AND ACCELERATING IN TWO-SECTION TECHNOLOGICAL LINAC

*N.I. Aizatsky, I.V. Khodak, V.A. Kushnir, V.V. Mitrochenko, S.A. Perezhugin
National Science Center "Kharkov Institute of Physics and Technology",
"Accelerator" R&D Production Establishment, Kharkov, Ukraine*

The paper presents the results of electron dynamics computing in the powerful resonance electron accelerator. The accelerator consists of two accelerating structures with a variable geometry and an injector including a diode electron gun, klystron type buncher and accelerating cavity. The wave phase velocity in structures is equal to the light velocity. The electron motion in the accelerator was simulated using the PARMELA code. With the 11 MW RF power supplying accelerating structures and the 1 A current at the accelerator exit the beam energy is up to 20 MeV.

PACS: 41.85

1. INTRODUCTION

Powerful linear electron accelerators with the energy up to 20 MeV can be applied for radiation technologies, for instance, for radionuclide production using (γ, n) reactions [1]. Such performances as the electron efficiency, accelerator length, probability of accelerating structures and beamline to be damaged by a beam and the reliability of a whole facility are important for a technological accelerator. The present paper is devoted to electron beam dynamics simulation in the one of such accelerator. Basing on a long-term operational experience the KUT accelerator [2] was selected as a prototype for the accelerator design. This accelerator consists of an injector and one accelerating section with the variable geometry and constant phase velocity. The injector includes diode electron gun, klystron type buncher and accelerating cavity. The length of the accelerating section is 1.2 m, the oscillation mode is $\Theta=2\pi/3$ at a frequency of 2797.2 MHz. The electron energy at its exit with the beam current 1 A can reach 10 MeV. It is supposed to use one more the same section to get the electron energy gain up to 20 MeV.

The purpose of simulation was the optimization of electron dynamics in the injector, calculation of beam parameters at the accelerator exit and calculation of operating performances, in particular, the dissipating power caused by lost particles.

2. SIMULATION METHODS

As the operating of the accelerator is supposed with long enough current pulse duration ($\sim 4 \mu\text{s}$) the only steady-state mode was considered on this stage of researches. Beam parameters at the gun [3] exit were calculated using the EGUN code [4]. The longitudinal and transverse beam dynamics in the accelerator was simulated using the PARMELA code [5]. This code computes the electron dynamics in the given electromagnetic fields. The space distribution of magnetic field in axial focusing magnetic elements of the accelerator (three lenses and a short solenoid on the first section) and the space distribution of

electromagnetic fields in the buncher and the accelerating cavity were computed using the SUPERFISH/POISSON code [6]. This code was also used for the space harmonics computing in the piecewise uniform structure (11 harmonics were taken into account). The calculation of amplitude and phase distribution for the fundamental space harmonic in the non-uniform structure, with taking into account the current loading, was performed using a self-consistent one-dimensional model [7] by dividing the interaction region into an arrange of uniform sites matching to each other on an operating frequency. The energy and the bunch phase length at the structure input were calculated using results of the injector PARMELA simulation. Results of the self-consistent problem calculation were used to evaluate the amplitude and phase of fundamental space harmonic in each cell of the travelling wave (TW) accelerating structure as it is needed for PARMELA simulations. According to the code the travelling wave accelerating structure is represented by an arrange of cells which would be if the structure to be cut along transverse planes at the middle of disks except the first cell. The first cell has a length equal to half a length of the next cell. Therefore the structure begins from the half a cell that makes it possible to take into account field penetration in the input coupler. According to this, the input coupler is divided in two regions. The first region is the first TW cell. The second one is the cavity completing this cell to the real coupler. As the field at the structure exit in operating mode is small enough the output coupler is set as a simple cell of the structure. Fig. 1 indicates the instantaneous electric field distribution along the axis of the first structure proceeding from spatial harmonics computing for 10 MW input power and 1 A beam current.

To take correctly into account the space charge forces the beam is set as a bunch having the length $5\beta\lambda$, where β is the initial normalized velocity of particles, λ is the operating wavelength.

3. SIMULATION RESULTS

The simulation has been carried out in several steps. During the first step there was investigated beam parameters at the injector exit depending on the phase shift between the buncher and accelerating cavity and on the field amplitude in the accelerating cavity under different magnetic field configurations and positions of elements of the injector. Based on simulation results the injector layout was optimized. Fig. 2 and 3 indicate some simulation results of particle dynamics in the upgraded injector.

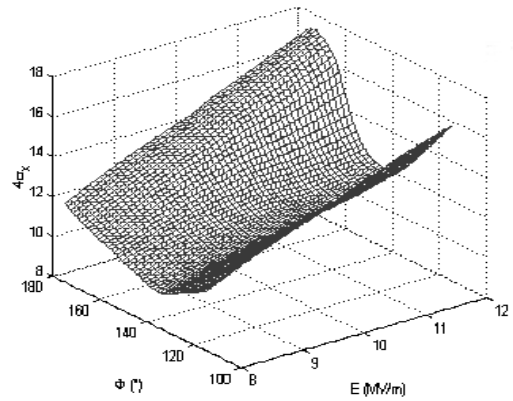


Fig. 3. Beam diameter at the injector exit (95% of particles)

The phase length of the bunch containing 70 % of particles and the beam diameter (95 % of particles) are shown as a function of a phase shift and average field strength in the accelerating cavity. Proceeding from the obtained results and accessible 1 MW RF power the best values of phase shift and field amplitude in the accelerating cavity are selected ($\phi=150^\circ$ and $E = 10$ MV/m).

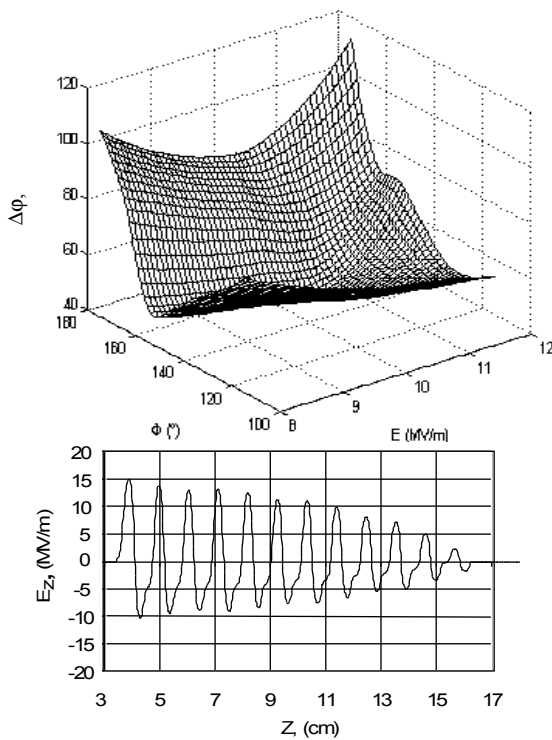


Fig. 1. Instantaneous electric field distribution along axis of the first section

Fig. 2. Bunch phase length at the injector exit (of 70 particles).

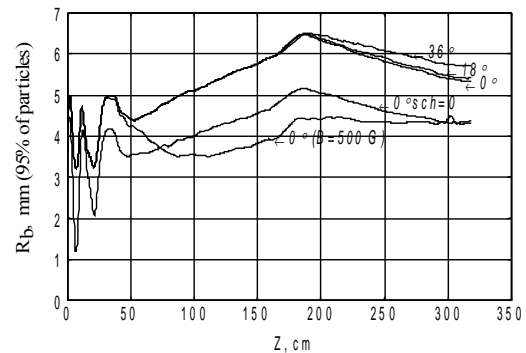


Fig. 4. Beam envelope along the accelerator

In the next step the first accelerating section was added to the injector and the phase shift between them giving the maximum energy gain was computed. Then the second section was added and the same procedure was carried out for the phase shift between sections. Fig. 4 shows the envelope of the beam containing 95 % of particles along the accelerator with different phase shifts between sections. The solenoid was turned off in this case. The curve marked "0°" corresponds to the maximum energy gain of a bunch. The curve marked "sch=0" corresponds to the simulation without taking into account the space charge forces. The curve marked "0° (B=500 G)" is obtained in the case when the solenoid was turned on with a 500 G field. One can see that the section has a RF focusing. The beam diameter is less than the minimum aperture of the section ($\varnothing = 19$ mm) even though the solenoid is turned off. It should be noted that it is necessary to be careful choosing the solenoid field on the first section of such two-section accelerator because the beam overfocusing can damage elements of a target part of the accelerator.

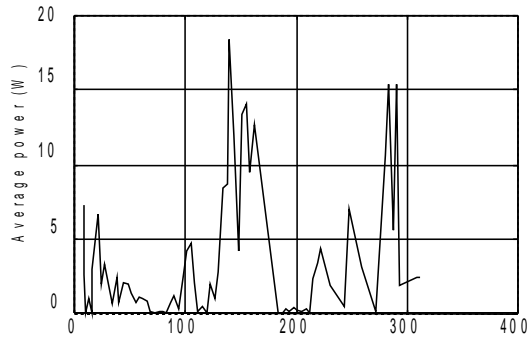


Fig. 5. Average dissipating power distribution along the accelerator

Fig. 5 shows the average dissipating power distribution along the accelerator (duty factor was equal to 0.1%). Such dissipating power does not represent a danger to the accelerator elements. The main part of particles (26 %) is lost in the injector, 10 % of particles are lost in the first section and 1 % is lost in the second section. Therewith the main energy loss falls at the first diaphragm of the subsection with a minimum aperture magnitude. The average power released in it will be 18 W.

Table 1

Parameters	Out cav.	Incoming section
P_{in} , MW ($I_{gun}=1,54A$)	1	--
I_{out} , A	1,18	1.14
$\epsilon_{x\ rms}$, π -mm-mrad (norm)	54	86
$\epsilon_{y\ rms}$, π -mm-mrad (norm)	53	90
$4\sigma_x$, mm	6.6	10
$4\sigma_y$, mm	6.3	10
$\Delta\phi$ for 70% of particles	26	39
$\Delta W/W$, % for 70% of particles	20	19
W_{max} , MeV	0.61	0.61
W_{av} , MeV	0.49	0.51
$W_{max\ probability}$, MeV	0.55	0.6
\varnothing_x , mm for 70% of particles	2.6	4.5
\varnothing_y , mm for 70% of particles	2.6	4.4

Table 2

Parameters	Section #1	Section #2
P_{in} , MW	11	11
I_{out} , A	1,04	1,0
$\epsilon_{x\ rms}$, π -mm-mrad (norm.)	48	46
$\epsilon_{y\ rms}$, π -mm-mrad (norm.)	48	45
$4\sigma_x$, mm (B=0)	8.9 (13)	8.8 (10,7)
$4\sigma_y$, mm (B=0)	8.9 (13)	8.8 (10,7)
$\Delta\phi$ for 70 % of particles	22	21
$\Delta W/W$, % for 70 % of particles	5	3
W_{max} , MeV	10.1	19.8
W_{av} , MeV	9.4	18.9
$W_{max\ probability}$, MeV	10	19.8

\varnothing_x , mm (B=0) for 70 % of particles	3.6 (6)	3.4 (5)
\varnothing_y , mm (B=0) for 70 % of particles	3.3 (6)	3.4 (5)

Analysis of the transverse beam profile at the accelerator exit showed the beam has a brightly expressed core. The beam parameters at the injector and at the exit of sections are given in Table 1 and Table 2, respectively. The beam FWHM is 2.5 mm in diameter (beam sizes for 70 % and 95 % of particles are indicated in Table 2). Therewith the beam has a halo limited by the aperture of the accelerator. The average power of 258 W (178 W in the first section with the injector and 82 W in the second section) will dissipate in the accelerator because of halo particle losing. It will be about 1 % from the average power of the accelerated beam.

4. CONCLUSION

The fulfilled beam dynamics simulation showed the availability of the chosen accelerator design. Simulation results allowed chan the injector and electron gun layout for improvement of the beam parameters at the accelerator exit. According to the simulation the capture ratio in the accelerator will be up to 66 % with the average beam power about 20 kW.

Therewith the questions concerned with dynamics in unsteady-state mode and in axial nonsymmetrical electromagnetic fields require the further researches.

REFERENCES

1. A.N. Dovbnya, G.D. Pugachev, D.G. Pugachev et. al. Obtaining power photon beams for medical radionuclidous production // *VANT, "Nuclear Physics Research" series*, 1997, v. 4,5(31,32), p. 154 – 156 (in Russian).
2. N.I. Aizatsky, Yu.I. Akchurin, V.A., Gurin et. al. KUT-industrial technological acceleretor // *Proceedings of XIV Workshop on charged particles accelerators*, Protvino, 1994, v. 4, p. 259-263 (in Russian).
3. I.V. Khodak, V.A. Kushnir, V.V. Mitrochenko et. al. Electron gun for technological linear accelerator // *VANT, this issue*, p.86-88.
4. W.B. Herrmannsfeldt. *EGUN: Electron Optics Program*, Stanford Linear Accelerator Center, SLAC-PUB-6729, 1994.
5. L.M. Young. *PARMELA*. –Los Alamos, 1996, p. 93 (preprint) / Los Alamos National Laboratory, LA-UR-96-1835).
6. J.H. Billen and L.M. Young. POISSON/SUPERFISH on PC compatibles // *Proc. 1993 Particle Accelerator Conf., Washington (USA)*, 1993, p. 790–792.
7. N.I. Aizatsky, L.A. Makhnenko. About current loading of the bunching section of a linear accelerator, *GTF*, 1982, v. 52, Ser. 4, p. 680-683 (in Russian).